The Stress State of Corner Cutout Area of the Model Boundary by Photoelastic Method

Lyudmila Frishter

Abstract The stress–strain state in the zone of the corner cutout of the area boundary is characterized by the singularity of the solution of the homogeneous boundary value problem and the complexity of its analysis. This article focuses on the stress state (SS) in the neighborhood of an irregular point of the area boundary on flat composite models with different cutout angles of the polymer material end. Forced deformations are created in one of the areas of the model, the forced deformations gap along the area contact boundary extends to the top of the corner cutout on the boundary of the model. The solution is obtained by means of experiments on optically sensitive material models by photoelastic method using the free temperature deformation defrosting property. A comparison of the SS obtained experimentally on the model and the parent distribution of SS in the zone adjacent to the irregular point of the area boundary is given. A conclusion is made on coincidence of the positions of the pure shear line obtained experimentally on the model and the neutral axis for the corresponding wedge under the action of a concentrated load. This paper is aimed at analyzing SS in the zone of the corner cutout of the boundary of the region and identifying the self-balanced SS corresponding to the solution of the homogeneous boundary value problem in the area with an irregular boundary point.

Keywords Stress state · Corner cutout of the area boundary · Photoelastic method · Singularity of the solution

1 Introduction

The stress–strain state (SSS) of composite structures is characterized by the concentration of stresses at the junctions of elements with different design of the boundary: special lines, points, such as the reentrant angle, etc. The complex SSS occurs in the stress concentration area, which is due to the shape of the boundary or "geometric

L. Frishter (✉)
National Research University Moscow State University of Civil Engineering, 26 Yaroslavskoye Shosse, 129337 Moscow, Russian Federation

A. Beskopylny and M. Shamtsyan (eds.), *XIV International Scientific Conference "INTERAGROMASH 2021"*, Lecture Notes in Networks and Systems 247,
https://doi.org/10.1007/978-3-030-80946-1_8

factor" and the finite discontinuity of the given forced strains, mechanical properties, going out to an irregular point of the area boundary. The complexity of the SSS analysis in the corner cutout zone of the area boundary is due to the singularity of the solution of the homogeneous boundary value problem of elasticity.

The solution of elliptic equations for areas with non-smooth boundaries is considered in papers of Williams, Kondratiev, Fufaev, Ufliand, Kalandiia, Cherepanov [1], Bodzhi, Aksentian, Aleksandrova, Chobanian. In papers [1–7], the stress nature in the corner zone of a plane wedge for different boundary conditions on its sides is determined. In the neighborhood of irregular boundary points, the solution of the elliptic boundary value problem is given in the form of asymptotic series and an infinitely differentiable function. The components of these series contain solutions of homogeneous boundary value problems for model areas: a cone or a wedge. These solutions depend on local characteristics: the values of the solid and plane angle and the type of boundary conditions [7–14]. The values of the solution expansion coefficients in the neighborhood of the singular point are unknown and depend on the problem as a whole.

The application of the well-known experimental photoelastic method [9, 15–20] makes it possible to obtain a solution of the elasticity problem on the model with a corner cutout of the boundary. The most developed and effective is the method for solving plane problems of deformable body mechanics [9, 20].

Experimentally, the stress state in the neighborhood of an irregular point of the boundary area is obtained by photoelastic method using the free temperature deformation defrosting property [12, 15–20] on flat composite polymer models with different cutout corners of the boundary. Forced deformations are created in one of the areas of the model, the forced deformations gap along the area contact boundary extends to the top of the corner cutout on the boundary of the model.

This paper is aimed at analyzing SS in the zone of the corner cutout of the boundary of the region and identifying the self-balanced SS corresponding to the solution of the homogeneous boundary value problem in the area with an irregular boundary point.

2 Materials and Methods

2.1 Experimental Solution of the Boundary Corner Cutout Problem on a Flat Model by Photoelastic Method

An experimental solution of a plane problem for an area with a cutout at the boundary, the geometry of which causes the occurrence of stress concentration, is considered.

The plane area consists of parts Ω_1 and Ω_2, with elasticity module E, Poisson's material ratio ν and linear expansion coefficient α. Temperature deformations $\alpha T \delta_{ij}$ are created in one of the areas—Ω_2, the area Ω_1 is not loaded. Along the area contact line $\Gamma = \Omega_1 \cap \Omega_2$, there is a deformation jump $\Delta\varepsilon_{ij} = \alpha T \delta_{ij}$, which goes to the body

boundary S to the point $O(0, 0)$—the top of the corner cutout of the area boundary. For different angles of the corner cutout solution of the boundary at its top, there is a feature of the stress state, which is experimentally realized on the model made of optically sensitive material as a stress raiser (see Fig. 1).

The elastic problem under the action of temperature deformations is solved by the photoelastic method using the property of "defrosting" of free temperature deformations [12, 16, 20]. A model of homogeneous epoxy material with given dimensions l = 180 mm, h = 25(23) mm is glued from two elements. The Ω_2 area element is cut from a plate obtained from the longitudinal shear of a hollow cylinder frozen under the action of a longitudinal uniformly distributed compression load. The height of the cylinder before "freezing" is H = 309 mm, the outer diameter is D = 180 mm, the inner diameter is 150 mm. The ends of the cylinder are cut off after freezing and only the middle part of the cylinder, which is in a flat deformed state, is considered. The compression of the cylinder after applying the load and freezing is $\Delta H = 9$ mm, relative elongation along the longitudinal axis OZ of the cylinder is $\varepsilon_z = \frac{\Delta H}{H} = \frac{9}{300} \approx 0.03$. Compression stress is

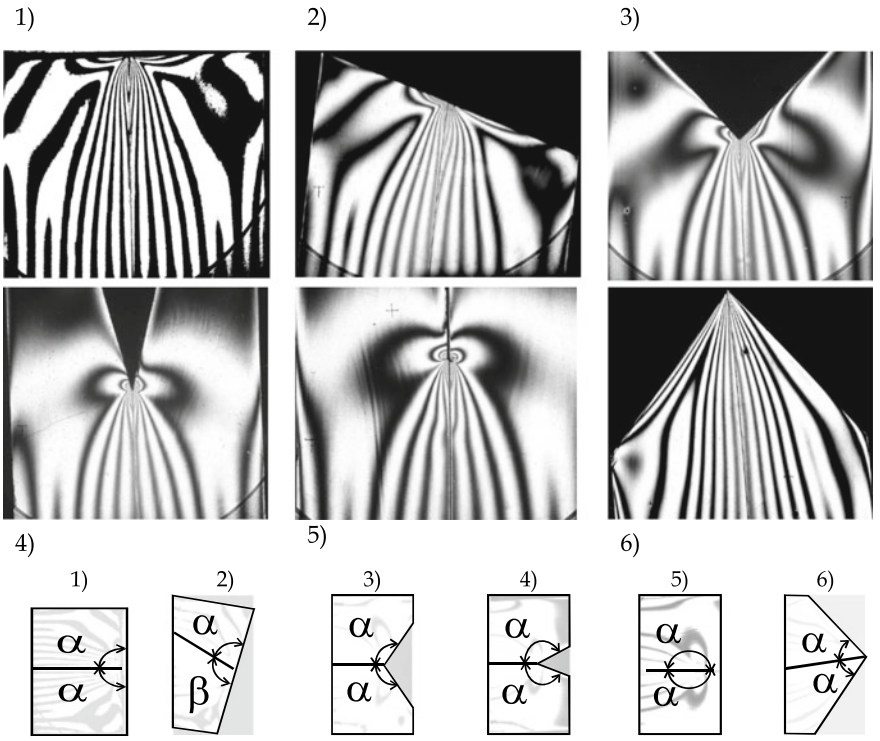

Fig. 1 Patterns of strips in models $t = 3$ mm thick for different cases of the model end solution: (1) $2\alpha = 180°$; (2) $\alpha + \beta = 180°$, $\alpha = 105°$, $\beta = 75°$; (3) $2\alpha = 270°$; (4) $2\alpha = 330°$; (5) $2\alpha = 360°$—narrow cutout—gap; (6) $2\alpha = 90°$

$\sigma_z = -\frac{P}{F} = -E\varepsilon_z = -200 \cdot 0.03 = -6$ kg/cm^2, $\sigma_z = \frac{\sigma^{1.0} m}{t} \Rightarrow m = \frac{\sigma_z \cdot t}{\sigma^{1.0}}$, where t is a shear thickness; $\sigma^{1.0}$ is a price of the model strip material; $\sigma^{1.0} = 0.341$. According to these data, in the shear $t = 0.3$ cm thick, the number of strips is $m = 5.3$.

The area Ω_1 is cut from free unloaded material. The areas Ω_1 and Ω_2 are glued together, then the model is "defrosted". The model generates SSS due to the action in the Ω_2 area of temperature deformations. $\varepsilon_0 = -\varepsilon_z = -\alpha T \delta_{ij}$.

The pattern of the strips corresponding to the stress–strain state from the action of temperature deformations for different shapes of the model end boundary is shown in Fig. 1. Model thickness (1)…(6) is the same and equals to $t = 3$ mm. In case (6), stress concentration at the top of point $O(0, 0)$ is not observed and stresses at the very top $O(0, 0)$ are zero.

2.2 *Analysis of the Stress State Obtained Experimentally on the Photoelastic Method Model*

The solution obtained experimentally on the composite model in the area of the corner cutout of the boundary under the action of discontinuous forced deformations is analyzed. An irregular point of the area boundary is considered as a top of the cutout of the end of the flat model lying on the contact boundary of the model parts.

We consider the neighborhood of an irregular point of the boundary adjacent to the singular point from which the irregular point is removed. Experimentally, the singular area on the model is defined as the neighborhood of the top of the corner cutout of the boundary, in which the interference fringes are blurred and the isochrome picture is not readable at any magnification of the neighborhood fragment.

The stress state in the neighborhood of the irregular point of the model boundary can be represented as Areas I, II, III according to Fig. 2a, where, due to the oblique symmetry of the stress diagrams, one of the areas Ω_2 is given.

Area I is an area adjacent to the symmetry axis of the model Γ: $y = 0$, where the main compressive stresses σ_2 considerably exceed the modulus of the main tensile stresses σ_1. As the point moves away from the top of the cutout in area I, the σ_1 stresses nature may change from tensile to compressive.

The main vector on the radial sites at the points of the area I (see Fig. 1a) has a normal component $\sigma_i = \sigma_r$ considerably superior in modulo to the tangential one σ_θ, which agrees with the ratio of the values of the principal stresses: $|\sigma_2| \gg \sigma_1$; $\sigma_1 \to 0$ at $(x, y) \to (x, 0)$; $\sigma_1|\Gamma = 0$; $\Gamma: y = 0$.

Area III is the area adjacent to the model cutout boundary, where the tensile principal stresses σ_1 considerably exceed the modulus of compressive stresses σ_2: $\sigma_1 \gg |\sigma_2|$; $\sigma_2 \to 0$ at $(x, y) \to S$; S—model boundary; $S: y = ax$, $a = tg\alpha$, 2α—angle of the model end opening; $\sigma_2|S = 0$.

Area II is a transitional area in which sharp angles, isochrome and significant gradients of the isocline parameter forming loops are observed. The largest isocline

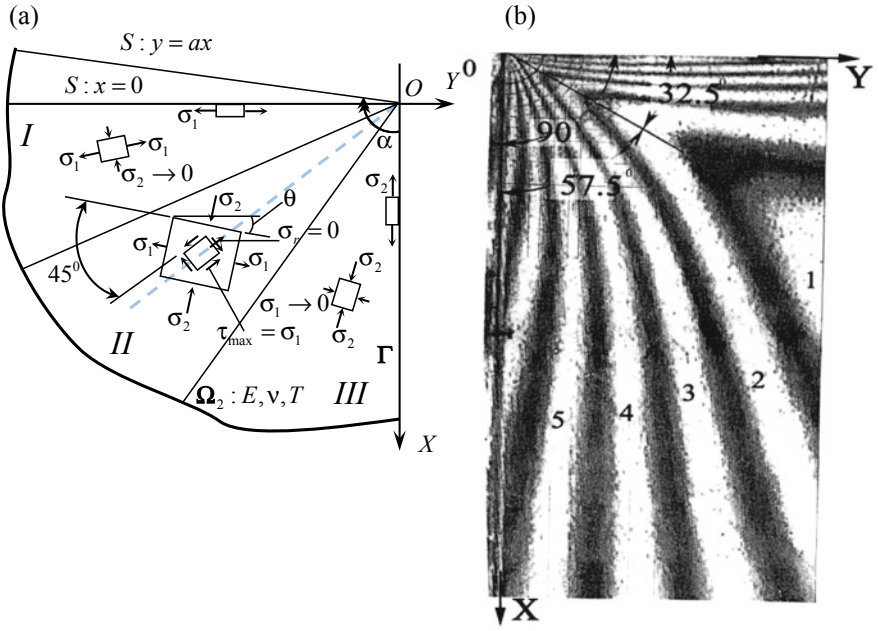

Fig. 2 SS scheme in the neighborhood of an irregular point of the boundary of a plane area. – – – —pure shear line

parameter is observed for the inner, nested in the remaining isocline loops, and varies from 45°…50° up to 70° when increasing the opening of the model end from $2\alpha = 180°$ to $2\alpha = 260°$.

There is a change in the direction of the main sites rotation in area II. If the main sites rotate clockwise in area III, then, passing area II, they change the direction of rotation to the opposite, so that the rotation of the main sites at the points of area I is observed in a clockwise direction as before.

In the transition area II (see Fig. 2a), a pure shear site is observed. The principal stresses at these points are equal in modulo and opposite in sign: $\sigma_1 = -\sigma_2$. The sites tilted at an angle of 45° to the main ones are in pure shear conditions, i.e. $\tau_{\max} = \frac{\sigma_1 - \sigma_2}{2} = \sigma_1$, and the normal stresses across these sites are zero: $\sigma_i = \frac{(\sigma_1 + \sigma_2)}{2} = 0$. According to the experimental data, the pure shear sites coincide with the radial ones. The radial stress as the normal stress over the pure shear site is zero: $\sigma_r = 0$, and shear stresses $\tau_{\max} = \frac{m\sigma^{1.0}}{2t} \neq 0$. Therefore, the isochrome orders m at the points of pure shear sites are not equal to zero. According to the experimental data, pure shear sites are observed at the tops of sharp angles of isochromes and their vicinities.

The stresses are continuous in the area $\Omega_2: 0 \leq \theta \leq \alpha$, so there is a subarea in transition area II in which pure shear and a stress state close to it are observed. For this "pure shear" subarea, there are sites where the normal stresses coincide or are close to the radial stresses and are equal or close to zero: $\sigma_i \cong \sigma_r \cong 0$ (see Fig. 2).

Main stresses σ_2 continuously varying from the highest value along the contact line of the area Γ: y = 0 in area I, going to area II "pure shear" subarea, then quickly decrease to zero values in area III. The sign may also change for main stresses σ_2 when approaching the boundary of the area S. Similar, tensile stresses σ_1, changing continuously from the highest values at the model cutout boundary in area III, passing to the "pure shear" subarea II, then rapidly decreasing to zero values in area I. For the main stresses σ_1 the sign may also change at the transition to the area contact line $\Gamma = \Omega_1 \cap \Omega_2$, Γ: y = 0.

Radial stresses in area I: $\sigma_r \cong \sigma_2$ at $(x, y) \to (x, 0)$, and in area III: $\sigma_r \cong \sigma_1$ at $(x, y) \to (x, \alpha x)$, S: $y = ax$, $a = tg\alpha$. In the transition area II on pure shear sites and close to them $\sigma_r = 0$ or $\sigma_r \approx 0$. Such a distribution of radial stresses in the neighborhood of the top of the model end cutout corresponds to the theoretical radial stress distribution of the form:

$$\sigma_r = cf(r)f(\theta) = \frac{\alpha ET}{r^{1-\lambda}}(c_1 \cos\theta + c_2 \sin\theta),\ \sigma_\theta = \tau_{r\theta} = 0 \tag{1}$$

At the pure shear sites, at $\theta = \theta_0$, $r > r_0$, r_0—sufficiently small, $\sigma_r = 0$, $\sigma_r = \frac{\alpha ET}{r^{1-\lambda_0}}(c_1 \cos\theta_0 + c_2 \sin\theta_0) = 0 \Rightarrow c_1 = -c_2\left(\frac{\sin\theta_0}{\cos\theta_0}\right)$.

The theoretical radial distribution of stresses in the neighborhood of the cutout of the model of the form (1) is understood as a self-balanced "own" stress state in the neighborhood of an irregular border point obtained as a solution of a plane homogeneous boundary value problem.

2.3 *Example of Stress State Analysis Obtained on a Flat Model with a Straight End*

The stress state is analyzed in the neighborhood of the irregular point of the boundary where the gap of forced deformations exits, using the straight end model as an example. According to the theoretical model [1–4, 12, 13], the stress state in the neighborhood of an irregular point of the area boundary can be represented as:

$$\sigma_{ij} = \sigma_{ij}^o + \sigma_{ij}^l \tag{2}$$

where σ_{ij}—stresses in the vicinity of an irregular point of the area boundary; σ_{ij}^o—eigensolution of the homogeneous boundary value problem in the vicinity of an irregular boundary point; σ_{ij}^l—stress caused by the action of the specified loads or the total stress field.

Internal stresses σ_{ij}^o in the area of the end of the model with a straight end have a radial view [1–4, 12, 13]:

$$\sigma_r = \frac{\alpha ET}{r}(c_1 \cos\theta_0 + c_2 \sin\theta_0), \quad \sigma_\theta = \tau_{r\theta} = 0 \tag{3}$$

With a continuous distribution of stresses in the area Ω_2 (similarly in the area Ω_1) of the form (3) in the cross-section $r = r_0$ there will be a point at which $\sigma_r = 0$. Consider one area of the straight-end model, for example, Ω_2: E, ν, αT. Pattern of the model strips for the area Ω_2 is given in Fig. 2b. According to the experimental data in area II of the model, the point with the net shear area is observed in the cross section at an angle $\theta_0 \approx 60°$. Figure 2 shows the "pure shear" line, which has a slope angle $\theta_0 \approx 57.5°$ in the vicinity of point $O(0, 0)$. According to the experimental findings

$$\sigma_r = 0 \text{ at } \theta_0 \approx 57.5° \tag{4}$$

Taking into account the theoretical distribution (1), the radial stresses will be recorded:

$$\sigma_r = \frac{c_0}{r}(c_1 \cos\theta + c_2 \sin\theta) = 0, \tag{5}$$

or

$$c_1 = -c_2 \frac{\sin\theta_0}{\cos\theta_0} = -c_2 \frac{\sin 57.5°}{\cos 57.5°} = -1.57c_2 \tag{6}$$

Stress (3) taking into account (6) will write over:

$$\sigma_r = \frac{c}{r}(-1.57\cos\theta + \sin\theta) \tag{7}$$

where $c = c_0\, c_2$, c is an unknown multiplier.

Determine what force is statically equivalent to the radial stresses (7), acting over a small radius cross section $r = r_0$ of the area Ω_2 of the model end [4, 12, 16, 17].

$$P_V = \sum X = \int_0^{\frac{\pi}{2}} \sigma_r \cos\theta \mathrm{d}F \;\; = \int_0^{\frac{\pi}{2}} \sigma_r \cos\theta r t \mathrm{d}\theta \tag{8}$$

where t is a model thickness. Considering (7), force P_V equals:

$$P_V = \int_0^{\frac{\pi}{2}} \frac{c}{r}[-1.57\cos\theta + \sin\theta]\ \cos\theta r\ t\mathrm{d}\theta \;\; = -\frac{ct}{r}(1.57\pi + 1) \tag{9}$$

Let's find the horizontal component of the acting forces:

$$P_H = \sum Y = \int_0^{\frac{\pi}{2}} \sigma_r \sin\theta\ \mathrm{d}F \;\; = \int_0^{\frac{\pi}{2}} \sigma_r \sin\theta r t \mathrm{d}\theta \tag{10}$$

Considering (7), force P_H equals zero:

$$P_H = \int_0^{\frac{\pi}{2}} \frac{c}{r}(-1.57\cos\theta + \sin\theta)\sin\theta r t \mathrm{d}\theta = 0 \tag{11}$$

Then force action angle γ, statically equivalent to radial stresses of the form (7) in the area Ω_2: $tg\gamma = \frac{P_H}{P_V} = 0 \rightarrow \gamma = 0^0$.

Finally, the radial stresses of the form (7):

$$\sigma_r = \frac{c}{r}(-1.57\cos\theta + \sin\theta) \tag{12}$$

in the small radius cross section $r = r_0$ in the area Ω_2 are statically equivalent to the action of a vertical force directed along the axis OX:

$$P_V = \sum X = -\frac{ct}{4}(1.57\pi + 1) \tag{13}$$

and the horizontal thrust is zero: $P_H = \sum Y = 0$.

The resulting scheme of force action P_V, P_H in the small radius cross section $r = r_0$ of the model end coincides with the corresponding forces for the wedge with an opening angle $\theta = \frac{\pi}{2}$ under the action of a concentrated force at the top of the wedge [4, 12, 16, 17].

3 Results

The experimentally obtained position of the pure shear line in the irregular point area of the model boundary shows full coincidence with the position of the neutral axis of the radial stress state for the wedge in the area of the top $O(0, 0)$ under concentrated force action.

The coincidence of the slope angle of the pure shear line in the area of the model end and the neutral axis of the model wedge during the action of the radial stress state, the coincidence of the isocline parameter in the model isochrome tops and the calculated slope angle of the main sites confirm experimentally the existence of the self-balanced radial stress state in the neighborhood of the model end top, corresponding to the internal stress state σ_{ij}^o in the general presentation of the SS: $\sigma_{ij} = \sigma_{ij}^o + \sigma_{ij}^l$ of the model end.

4 Discussion

Experimentally, the singular area on the model is defined as the neighborhood of the top of the corner cutout of the boundary, in which the interference fringes are blurred and the isochrome pattern is not readable at any magnification of the neighborhood fragment. A contradiction arises with a continuous change of stresses in the punctured vicinity of an irregular boundary point, "sharp angles" of isochromes occur. The above analysis is applicable to the neighborhood of an irregular point of the boundary adjacent to the singular point from which the irregular point is removed. The validity of the analysis data in the selected area of the irregular boundary point is confirmed by the coincidence of the experimental and theoretical stress values.

5 Conclusions

The analysis of SS in the area of the irregular point of the boundary, in which the gap of forced deformations exits, shows the existence of a self-balanced SS σ_{ij}^{o}, corresponding to the solution of the homogeneous boundary value elasticity problem. It explains the growth of strips orders observed from the inside of the stress concentration area, and not at the very top of the cutout of the area. The inequation to zero of orders of the strips in area II of pure shear in the neighborhood of the top of the model end shows the existence of a self-balanced SS caused by the action of the given loads or the total stress field.

References

1. Cherepanov GN (2012) Fracture mechanics. Computer Research Institute, Izhevsk
2. Kuliev VD (2005) Singular boundary value problems. Nauka, Moscow
3. Feodosiev VI (2016) Strength of materials. Publ. House N. E. Bauman MSTU, Moscow
4. Parton V, Morozov E (2017) Elastic-plastic fracture mechanics: special problems of the fracture mechanics. Moscow
5. Bakushev SV (2013) Geometrically and physically nonlinear continuum mechanics. Plane problem. LIBROKOM, Moscow
6. Bakushev SV (2020) Differential equations and boundary value problems of deformable solid body mechanics. LENAND, Moscow
7. Matviyenko Yu (2006) Fracture mechanics models and criteria. Fizmatlit, Moscow
8. Albaut GN, Tabanjuhova MV, Harinova NV (2004) Determination of the first stress intensity factor in elements with angled cut-out. In: Experimental mechanics and calculation of structures (Kostinsky readings). Moscow State University Press, Moscow
9. Albaut GN, Kharinova NV, Sadovnichij VP, Semenova JI, Fedin SA (2011) Nonlinear problems of mechanics of destruction. Vestn Lobachevsky Univ Nizhni Novgorod 4:1344–1348
10. Vardanjan GS, Frishter LJu (2007) Int J Comput Civ Struct Eng 3:75–81
11. Pestrenin VM, Pestrenina IV, Landik LV (2013) Vestn TGU Math Mech 4:80–87
12. Razumovskij IA (2007) Interference-optical methods of deformable solid mechanics. Publisher MGTU named after N. Je. Bauman, Moscow, p 240

13. Frishter LYu (2017) Photoelasticity-based study of stress-strain state in the area of the plain domain boundary cut-out area vertex. In: Advances in intelligent systems and computing, EMMFT 2017, vol 692. Springer, pp 836–844
14. Makhutov NA, Moskvichev VV, Morozov EV, Goldstein RV (2017) Unification of computation and experimental methods of testing for crack resistance: development of the fracture mechanics and new goals. Ind Lab Diagn Mater 83(10):55–64
15. Kobayashi A (1990) Experimental mechanics, vol 1. Mir, Moscow, p 615; vol 2. Mir, Moscow, p 551
16. Hesin GL et al (1975) The photoelasticity method, vol 3. Stroyizdat, Moscow, p 311
17. Frocht MM (1948) Photoelasticity. In: Prigorovskiy NI (ed), vol 2. GITTL, Moscow, Leningrad
18. Durelli A, Riley W (1970) Introduction to photoelasticity. In: Prigorovskiy NI (ed). Mir, Moscow
19. Aleksandrov AJa, Ahmetzjanov MH (1974) Polarization-optical methods for deformable solid mechanics. Nauka, Moscow, p 576
20. Koshelenko AS, Poznjak GG (2004) Theoretical foundations and practice of photo mechanics in mechanical engineering. Granica, Moscow